International Journal of Sustainable and Green Energy
2025, Vol. 14, No. 3, pp. 160-170
https://doi.org/10.11648/j.ijsge.20251403.13

Research Article

Selective Allocation of Distributed Photovoltaic Systems Using Experimental Data from Tropical Areas

Kitmo*, Colbert Babé, Nisso Nicodem, Kola Bernard, Noël Djongyang

Department of Renewable Energy, National Advanced School of Engineering of Maroua, University of Maroua, Maroua, Cameroon

Abstract

In this study, the solar irradiance of four different localities in the Far North province of Cameroon was assessed with a view to selecting a site for a large-scale photovoltaic array. The global radiation extrapolation method is used to evaluate the solar potential in the four localities. To verify the reliability of the chosen method, the coefficient of determination is calculated to estimate the difference between the real-time experimental method and the theoretical method based on the statistical test. So, the Root Mean Square Error, the Mean Absolute Relative Error and the Coefficient of determination are calculated, in order to make a conjecture on the performance of the proposed method. The localities of Muidere, Bougaye, Youaye and Hoyo were chosen on the basis of the availability of sunlight in these areas. The results obtained also demonstrate the feasibility of implementing the system, taking into account the real data extracted from the site.

Keywords

Far North Province of Cameroon, Global Radiation, Data Acquisition, Distributed Photovoltaic Systems, Tropical Areas

1. Introduction

Although the world's population is growing every year, the use of fossil fuels is a danger to the life on our planet [1]. This consumption leads to atmospheric pollution, and even the depletion of these resources, making the price of oil unstable [2]. This is why we are encouraged to limit greenhouse gas emissions, which is why we are interested in renewable energies [3]. The aim of this article is firstly to assess the availability of solar energy, and secondly to investigate methods for estimating global solar radiation [4]. There are several methods for estimating solar radiation on the inclined and horizontal surfaces [5]. Some methods of estimating solar radiation or calibration are very costly [6]. However, the theoretical study of measurement data often presents certain inconsistencies, so in the work of [7], certain methods of solar radiation assessment are proposed. A review of the literature in [8] also presents the most widely used methods for extrapolating solar irradiance on the horizontal surface.

Recently [9], the method of extrapolating solar insolation on the inclined plane is proposed. Among the most widely used methods for estimating global solar radiation [10] are real-time machine learning algorithms, the use of meteorological data and the exploitation of geographical information on study areas. In previous work [11], a study is carried out on the evaluation of global solar radiation for the locality of Maroua [12]. This approach involved using and comparing empirical models of the results obtained. From this work, it

*Corresponding author: kitmobahn@gmail.com (Kitmo)

Received: 2 May 2025; **Accepted:** 23 June 2025; **Published:** 15 July 2025

was shown that it is during the dry season that the maximum values of photovoltaic solar power are produced [13]. Voltage profiles on the IEEE 33 bus showed that power grids into which 50MW of power is injected are stable during the dry season [14].

The study carried out [15] showed that the interconnected North Cameroon networks could be strengthened by the installation of a solar power plant in the Guider locality [16], which is why a photovoltaic power plant has been in operation there since 2022 [17]. In Cameroon's Far North region, a study showed that only 30% of the population has access to electricity [18], unlike other regions of the country [19]. And yet, the Far North region has an abundance of photovoltaic solar energy [20]. This is one of the regions where the literacy rate is too low [21], which justifies the fact that few people have access to electricity or the minimum of comfort. However, the development of any country in the world inevitably depends on access to drinking water and education [22]. Every year, the cholera epidemic is detected because populations have no access to drinking water [23]. On the other hand, access to healthcare is becoming more and more difficult, as the energy to run biomedical equipment is non-existent [24]. The only option the government offers the region is the use of thermal power plants, which provide intermittent, unstable electricity [25]. Delays and untimely power cuts are recurrent. These generators regularly break down. What's more, the diesel fuel used to run the thermal generators is very expensive and highly polluting [26]. This is a major issue that needs to be eradicated, as it hampers the country's socio-economic development and affects people's quality of life [27].

In this work, an experimental study based on real time data using performance indicators is carried out. Solar radiation is also estimated for the localities of Hoyo, Youaye, Bougaye and Muidere. Extrapolation of the photovoltaic solar power allows us to select the best locality for the implementation of a high-capacity photovoltaic power plant, in order to electrify the isolated and disadvantaged rural areas of the Far North region.

2. Experimental Setup for Data Acquisition

In order to make a comparative study and decide on the performance of the proposed method, Figure 1 depicts the system on which the meteorological data were processed. This diagram highlights the type of solar cell used. The data is first processed from NASA, and then the actual data is provided by the test bench set up in the four regions of the Extreme region. This experimental set-up makes it possible to get closer to reality and reduce calculation or estimation errors. The work in [28] shows that the polycrystalline cell is not suitable for the locality of guide given the fluctuation of the sunshine which remains inconstant for a whole day.

In the work of [29], monocrystalline cells are used to evaluate solar irradiance in order to meet the energy demand of the locality of Youaye. In the locality of Hoyo, a polycrystalline cell is used for an experimental study to produce photovoltaic solar energy to supply the locality of 154 households. Studies in the works of [30] show that the Far North region is suitable for the use of the polycrystalline cell, given the availability of education. However, theoretical data are not sufficient to reach a conjecture, so in this work real data supplied from acquisition benches are used to calculate the squared error in order to make a choice about the ideal locality. Other methods are associated with this test bench to optimize the proposed system. These include DC power conversion systems such as boost choppers, two-level inverters and active filters. The power of the photovoltaic generator is extrapolated by means of a duty cycle-controlled boost chopper. MPPT control [31] is used for this purpose.

Figure 1. *The setup platform of experimentation.*

3. Methodology

The methodological process used to evaluate the performance indicators of the proposed method and the extrapolation of photovoltaic power is based on the study of the values provided by the real-time data acquisition bench. After estimating solar radiation on the horizontal surface, the data extracted from the acquisition bench is used to assess calculation errors [32].

3.1. Estimation of the Solar Radiation

In order to determine solar radiation on the horizontal surface, the formula [33] is given in Equation (1). This formula is used to evaluate solar radiation on the horizontal surface and cannot be used when extrapolating solar radiation on the inclined surface.

$$H_{Ir} = \frac{24}{\pi} S_o \left[1 + 0.033\cos\left(\frac{360 S_d}{365}\right)\right] * \left[\cos\phi\cos\chi\sin\omega_s + \frac{2\pi\beta_{Sd}}{360}\sin\phi\sin\chi\right] \quad (1)$$

where χ and β_{Sd} are given by

$$\beta_{Sd} = \cos^{-1}\left(-\tan\phi\tan\chi\right) \quad (2)$$

$$\chi = 23.45\sin\left[\frac{360\left(284 + S_d\right)}{365}\right] \quad (3)$$

where S_o is the solar constant (W/m^2); β_{Sd} is the sunset hour angle (˚C); ϕ is the latitude of the location (˚) and μ, the solar declination (˚).

3.2. Modelling of the Photovoltaic System

The electrical circuit diagram in Figure 2 enables us to model the photovoltaic generator in MATLAB/Simulink, based on the mathematical equation [10]. The model features a diode, a shunt resistor R_P and a series resistor R_S. The R_P resistor is connected in parallel with a voltage source and a diode (D). Based on this single-diode model, the photovoltaic generator can be implemented in this software to obtain simulation results. Maximum power can be extracted from a photovoltaic source when the current is shaped by a chopper. The boost converter, for example, raises the output voltage level by controlling the duty cycle with MPPT control. Many heuristic algorithms are used to control such a DC/DC converter. In Equation (4) the variable Is represents the photo current generated. Maximum power can be extracted from a photovoltaic source when the current is shaped by a step-up buyer whose duty cycle is driven by the MPPT. Most heuristic algorithms are suitable for controlling such a DC converter. The value Is represents the photo current generated, which will be collected by the input of the DC/DC converter shown in Figure 3.

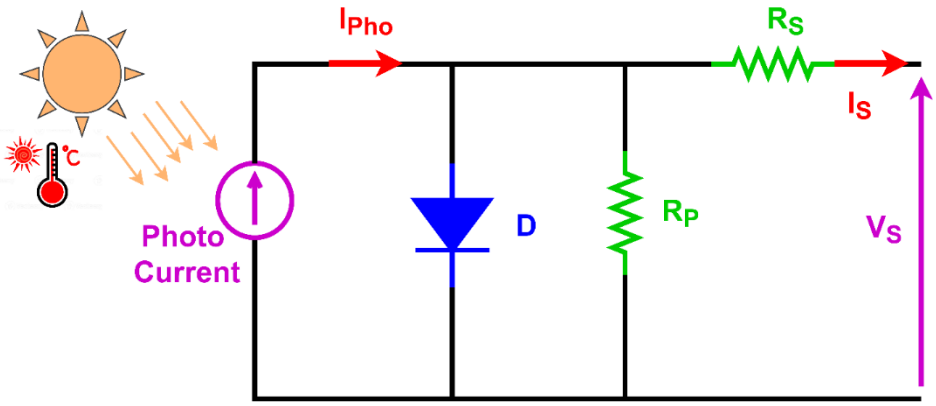

Figure 2. *Electrical circuit of PV source with one diode.*

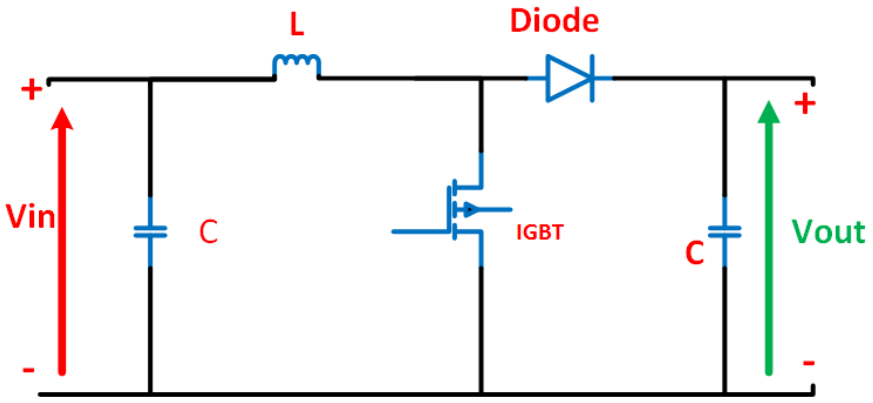

Figure 3. *Electrical circuit of boost chopper.*

$$I_s = I_{Pho} - I_0\left[exp\left(\frac{(V_s + R_S I_s)}{V_T A}\right) - 1\right] - \frac{V_s + R_S I_s}{R_P} \quad (4)$$

$$I_s = I_{Pho} - I_0\left[exp\left(\frac{q(V_s + R_S I_s)}{KTA}\right) - 1\right] - \frac{V_s + R_S I_s}{R_P} \quad (5)$$

Where $V_T = \frac{KT}{q}$

$$I_{Pho} = \left[I_{SC} + K_i\left(T - T_{ref}\right)\right]\frac{G}{G_n} \quad (6)$$

$$I_0 = I_{n,0}\left(\frac{T_{ref}^3}{T}\right)exp\left[\frac{qE_g}{AK}\left(\frac{1}{T_{ref}}-\frac{1}{T}\right)\right] \quad (7)$$

In Eq (4), the thermal voltage of the PV cell is V_T; I_{pho} is the Photo current generated due to incident solar irradiance; The reverse saturation current of the diode is represented by I_o;. The Boltzmann's constant is K=1.3806503 × 10−23 J/K. T is the Cell operating temperature in kelvin (K); q =1.60217646 × 10−19 C) represents the Charge of the electron; R_s: is the Series resistance representing an internal resistance of the PV cell (Ω). The parameter R_p is the Shunt resistance representing the leakage current of the PV cell (Ω); here the parameter A is the Diode ideality factor; I_{sc} is the shunt circuit current of the cell at 25 ℃ and 1,000 W/m^2; K_i is the temperature coefficient of the cell at I_{sc}. T_{ref}: represents the reference temperature of the cell; and G is the Solar irradiation (W/m^2). G_n the nominal solar irradiation; $I_{n,0}$ is the nominal saturation current and E_g represents the semiconductor energy band gap which is equal to E_g = 1.12eV, considering the polycrystalline silicon cell at 25 ℃.

4. Validation of the Method

Some performance indicators [34] can be used to demonstrate the reliability and credibility of a model. These include RMSE, MBE, MARE, MAE and R^2, commonly known as the coefficient of determination, which is the square of the correlation coefficient.

4.1. Evaluation of the Root Mean Square Error (RMSE)

One of the key parameters in evaluating the performance of a model is the RMSE, which is given in Equation (8). Calculating this parameter allows us to determine whether an approach or method is adequate when this value is as small as possible, i.e., close to zero. We assume that the method used to estimate a value is better if the result obtained offers a negligible value close to zero.

$$\text{RMSE} = \sqrt{\frac{1}{\gamma}\sum_{t=1}^{\gamma}\left(\overline{S}_{t,x}-\overline{S}_{t,y}\right)^2} \quad (8)$$

In this formula, γ is the size of data, $S_{t,x}$ is the measured data, $S_{t,y}$ is the experimental data. $\overline{S}_{t,x}$ and $\overline{S}_{t,y}$ are respectively their mean values.

4.2. Evaluation of the Mean Bias Error (MBE)

The MBE given in Equation (9) can also be used as a parameter to determine the performance or reliability of a model. When the MBE value is close to zero, then it is assumed that the model can be adopted. When this value is too large, there is overestimation of the data in the use of this model. On the other hand, when the MBE value is negative or too small, then this model makes an underestimation of input data.

$$\text{MBE} = \frac{1}{\gamma}\sum_{t=1}^{\gamma}\left(\overline{S}_{t,x}-\overline{S}_{t,y}\right) \quad (9)$$

4.3. Evaluation of the Mean Absolute Error (MAE)

Among the tools of your statistics, we also find the MAE which is an essential parameter in the evaluation of the performance of a model. For model validation, some prefer to use the MAE parameter, given in Equation (10), which gives a better precision than the RMSE. This parameter allows to have an idea on the details between two values, because the estimation step is reduced. When the sampling step is small, it is possible to have more details on the different continuous information in this interval; this is why many works have shown the superiority of this parameter on the RMSE.

$$\text{MAE} = \frac{1}{\gamma}\sum_{t=1}^{\gamma}\left|\overline{S}_{t,x}-\overline{S}_{t,y}\right| \quad (10)$$

4.4. Evaluation of the Mean Absolute Relative Error (MARE)

The MARE evaluation parameter can also be used to evaluate the performance of methods or models in estimating or extrapolating statistical data. It is considered as the absolute value of the mean of the predicted data over the experimental data. The Equation (11) gives this formula.

$$\text{MARE} = \frac{1}{\gamma}\sum_{t=1}^{\gamma}\left|\frac{\overline{S}_{t,x}-\overline{S}_{t,y}}{\overline{S}_{t,x}}\right| \quad (11)$$

4.5. Evaluation of the Coefficient of Determination (R^2)

Among all the most used statistical tests in the literature, the R^2 parameter is much more used. A value of R^2 close to 1 shows that the model can be adopted. The closer this value is to 1, the better the model is, the less this value deviates from 1, the worse the model is. This value should not exceed 1. This performance indicator is used by most of the works on the evaluation of models or statistical methods. This parameter is given by Equation (12).

$$R^2 = 1-\frac{\sum_{t=1}^{\gamma}\left(\overline{S}_{t,x}-\overline{S}_{t,y}\right)^2}{\sum_{t=1}^{\gamma}\left(\overline{S}_{t,x}-\overline{S}_{x,mean}\right)^2} \quad (12)$$

5. Results and Discussion

The results obtained in this article are based firstly on the calculation of global insolation based on statistical tests, and secondly on the acquisition of real-time data from test benches set up in four different localities: Hoyo, Muidere, Youaye and Bougaye. The evaluation of the photovoltaic energy potential not only demonstrates the performance and relevance of the proposed method, but also enables us to determine the appropriate location for a photovoltaic power plant to meet the electrical energy demand of isolated localities in the Far North region.

The aim of the power estimate is to meet or find an alternative to the energy supplied by the interconnected North Cameroon networks, which are experiencing load shedding difficulties and untimely power cuts. Several localities in the Far North region do not have the possibility of having an average energy continuity of 15% [35]. Electricity is only available 5 days out of 30, and sometimes when it is available, it is unstable, preventing the supply of certain electrical equipment that consumes sufficient active energy. The results obtained in the various localities enable us to evaluate the coefficient of determination, to assess the error difference between the experimental model and the theoretical model, and to calculate the RMSE. Analysis of the results shows that the method is suitable for estimating sunshine for those who make locality, as the error is almost negligible. This is demonstrated by the R^2 value, which is close to 1.

5.1. Data Collected and Power Produced for the Locality of Bougaye

The real-time data acquisition bench has also made it possible to determine the various power profiles from January to December. Power levels were 150 kW and 260 kW respectively. From February to April, the sun shines slightly, as it does in October and November. Photovoltaic power remains constant from May to August. This power profile highlights the fact that sunshine levels remain almost constant, enabling us to optimize the photovoltaic energy that can be stored in the battery banks. This location offers the possibility of integrating electrical energy storage systems to increase or raise the power level in the event of increased demand, when the demand for electrical energy becomes greater than the supply of electrical energy. The power profiles in Figure 4 from the Bougaye locality therefore offer the best performance in terms of RMSE, MARE, MBE or R^2.

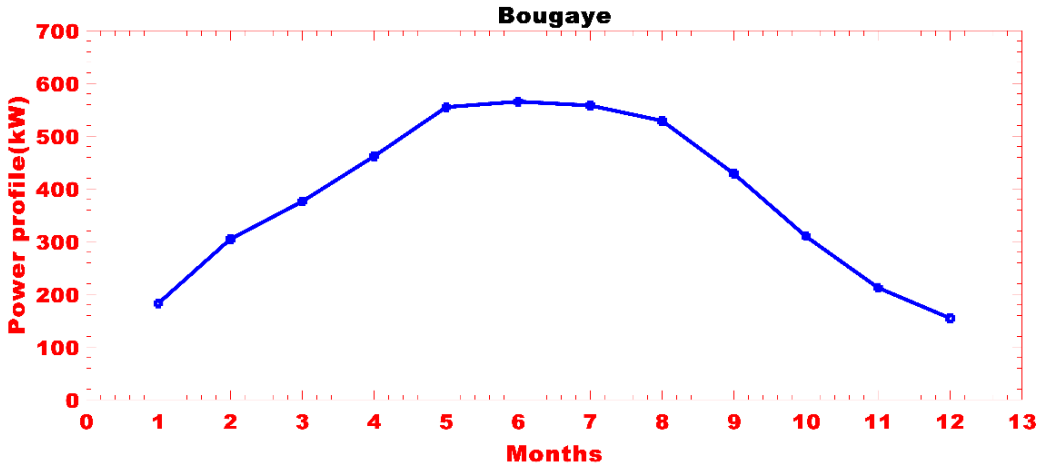

Figure 4. *The annual power profile from Bougaye locality.*

5.2. Data Collected and Power Produced for the Locality of Hoyo

Figure 5 shows the data supplied by the acquisition bench installed at the Hoyo site. The figure shows a power peak between June and July, when a power of 670 MW is observed. There is also a low level of power in January and December, corresponding to 170 kW and 180 kW respectively. In August and November, solar irradiation is almost negligible, and there is a drop in irradiation in the area.

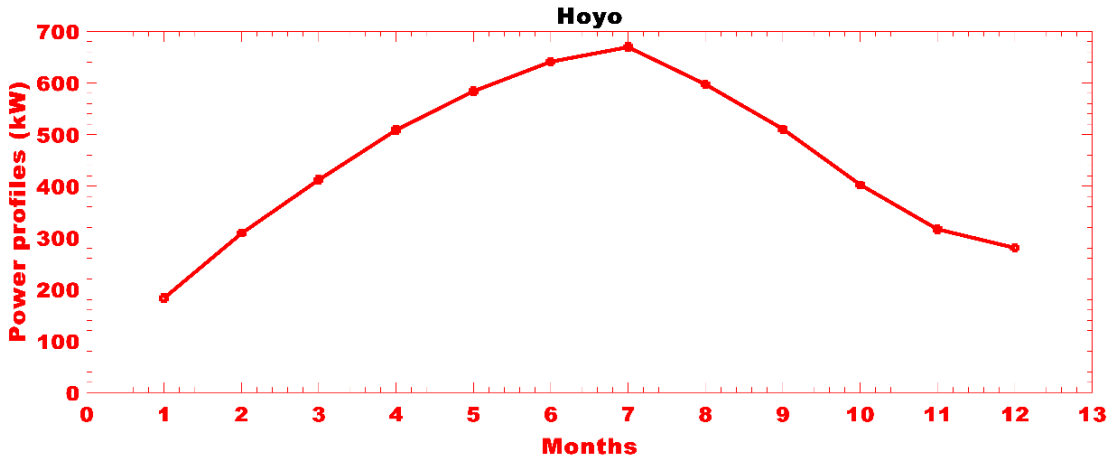

Figure 5. The annual power profile from Hoyo locality.

5.3. Data Collected and Power Produced for the Locality of Muidere

Many recent studies have focused on the evaluation of education in Muidere. In this study, an extrapolation of the solar photovoltaic power is made taking into account the meteorological data provided by the international airport of SALAK, located 200 km from Muidere. Using the extraction of numerical values obtained from the data acquisition bench, an extrapolation of the power is also made to bring out the power profile as described in Figure 6. This figure shows a high density of sunshine during the months of March, April and May. January and December, on the other hand, are less sunny. Based on these values, the power profile described in Figure 6 illustrates that a capacity of 0.25 MW can be generated for 6 months out of 12 in the locality of Muidere. This energy produced can supply the locality with electricity during times of load shedding or blackouts.

Figure 6. The annual power profile from Muidere locality.

5.4. Data Collected and Power Produced for the Locality of Youaye

The data provided by the test bench in Youaye show that a power rating of 6,80 kW is possible to supply a population with an electrical energy demand not exceeding 700 kW. On the one hand, this power profile highlights the abundance of sunshine in the locality of Youaye, and on the other, shows that it is possible to install a photovoltaic generator to meet this locality's demand. Figure 7 shows that power peaks are observed in June and July, corresponding to the amount of sunshine received at the surface of the solar panels. Sunshine levels are low around January and December, with active outputs of 180 kW and 220 kW respectively. This location therefore performs better in terms of indicators such as R2, RMSE, MAE, MBE and MARE.

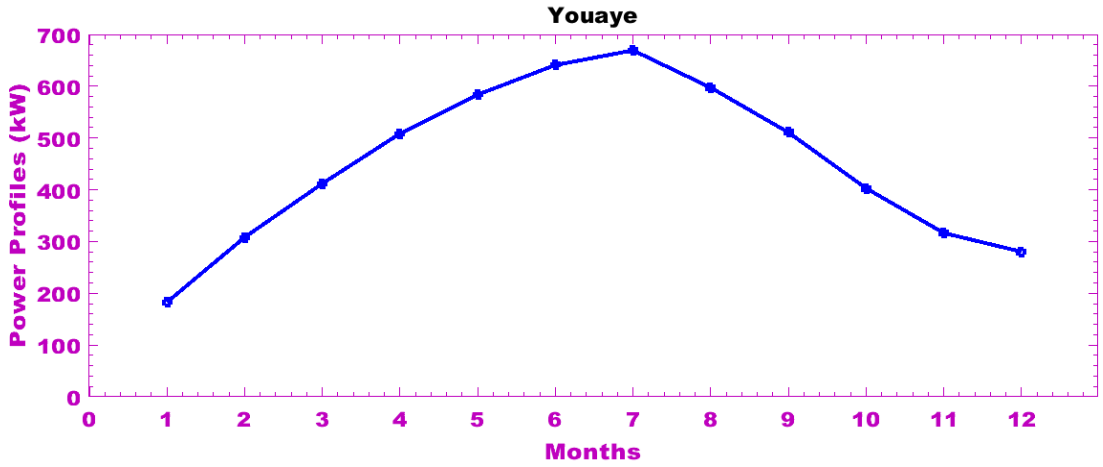

Figure 7. The annual power profile from Youaye locality.

6. Choice of the Selected Site

It is important to know the value of the coefficient of determination and of certain indicators such as the RMSE value to be able to make a conjecture about the efficiency of a model. In this section, these values are used to justify the power profiles or the extrapolation of photovoltaic solar power in the four selected localities. In this work, the four locations in the Far North region are chosen according to their abundance of sunshine. These tables show the various parameter values used to demonstrate the feasibility of the proposed model. Table 1 presents the values collected for the locality of Muidere, Table 2 shows the availability of the data collected for the locality of Bougaye, Table 3 provides the data for the locality of Youaye, while Table 4 presents the data for the locality of Hoyo. These data are calculated as weekly, monthly and annual averages. The values of the parameters of the R^2 coefficient of determination are also determined to make the conjecture on the model and to justify the availability of sunshine in this locality.

Table 1. Collected data from Muidere locality.

Muidere					
Months	**RMSE**	**MARE**	**MAE**	**MBE**	**R^2**
January	1.234	0.021	1.084	0.023	0.785
February	0.214	0.012	0.452	0.012	0.854
March	0.124	0.045	0.245	0.074	0.958
April	0.254	0.078	0.245	0.024	0.845
May	0.854	0.045	0.868	0.055	0.902
June	0.456	0.024	0.258	0.084	0.98
July	0.784	0.055	0.452	0.046	0.894
August	0.254	0.081	0.456	0.058	0.985
September	1.003	0.085	0.245	0.078	0.945
October	2.145	0.045	0.478	0.096	0.845
November	0.254	0.088	0.235	0.053	0.902
December	0.254	0.065	0.248	0.074	0.895

Table 2. Collected data from Bougaye locality.

Bougaye					
Months	**RMSE**	**MARE**	**MAE**	**MBE**	**R^2**
January	1.023	0.021	0.254	0.045	0.789
February	2.124	0.024	0.452	0.045	0.974
March	0.124	0.022	0.245	0.023	0.901
April	0.123	0.045	0.456	0.025	0.945
May	1.235	0.047	0.457	0.089	0.852
June	0.235	0.023	0.245	0.078	0.789
July	0.112	0.07	0.456	0.045	0.952
August	0.245	0.058	0.335	0.027	0.845
September	0.287	0.055	0.456	0.096	0.774
October	0.245	0.033	0.785	0.054	0.779
November	3.081	0.081	0.254	0.043	0.802
December	3.001	0.037	0.574	0.089	0.801

Table 3. Collected data from Youaye locality.

Youaye					
Months	**RMSE**	**MARE**	**MAE**	**MBE**	**R^2**
January	1.69	0.012	5.943	0.023	0.975
February	0.491	0.096	0.624	0.086	0.958
March	0.175	0.025	0.276	0.077	0.902
April	2.081	0.078	2.606	0.045	0.958
May	1.637	0.099	0.514	0.058	0.902
June	0.783	0.086	0.294	0.045	0.942
July	0.738	0.068	2.068	0.021	0.945
August	1.832	0.086	0.289	0.012	0.984
September	0.788	0.081	0.271	0.045	0.974
October	0.575	0.042	0.231	0.023	0.954
November	0.752	0.096	0.327	0.045	0.896
December	0.655	0.083	3.881	0.078	0.907

Table 4. Collected data from Hoyo locality.

Hoyo					
Months	**RMSE**	**MARE**	**MAE**	**MBE**	**R^2**
January	1.245	0.015	4.045	0.012	0.745
February	2.423	0.002	4.111	0.02	0.989
March	0.235	0.023	2.012	0.045	0.921
April	0.425	0.047	0.452	0.089	0.954
May	1.789	0.022	0.44	0.065	0.742
June	0.235	0.04	1.574	0.044	0.901
July	0.456	0.087	2.001	0.022	0.902
August	0.237	0.045	3.021	0.032	0. 968
September	2.478	0.077	0.444	0.011	0.981
October	1.356	0.056	0.234	0.045	0.785
November	3.587	0.065	0.785	0.085	0.979
December	0.412	0.023	3.456	0.074	0.881

7. Comparison of Power Profile of the Selected Localities

The results obtained in Figure 8 show that the locality of Youaye comes first with an electrical energy capacity of 7.6 MW, followed by the locality of Muidere, where an observed power of 6.2 MW is produced. Bougaye comes last, with an output of 5.2 MW, followed by Hoyo. These profiles of photovoltaic power generated by locality give an idea of the level of sunshine observed in the various localities where the test benches have been installed, with a view to obtaining real-time data. It can be seen that the Youaye locality offers the best yields in terms of the production of a photovoltaic energy capacity capable of meeting this locality's demand for electrical energy. Bougaye, on the other hand, is not a suitable location for a high-capacity photovoltaic power plant.

The average annual photovoltaic capacity of Youaye is 6MW, while Muidere is 5MW, and Hoyo and Bougaye are 5.2MW and 4.8MW respectively.

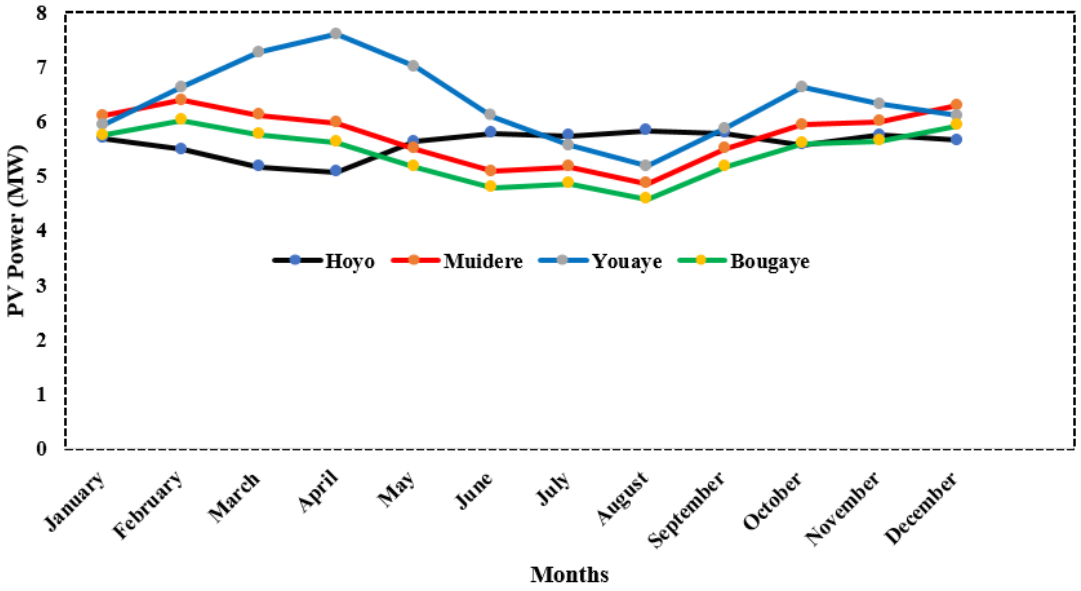

Figure 8. *The annual power profile of the selected localities.*

Finally, Table 5 shows the various performance parameter values collected to demonstrate the reliability of the proposed method. This table summarizes the different values of the performance indicators for the four selected localities. We can see that for the locality of Youaye gives a RMSE= 2.025 and a R^2 = 0.975. These parameters are necessary to select the best locality with the most sunshine. The Table 5 shows that Bougaye and Muidere are localities with low levels of sunshine and cannot be chosen for the implementation of a photovoltaic generator, as the population requires a lot of energy. The results obtained and contained in Table 5 allow us to conclude that not only are Hoyo's actual values inadequate to meet this locality's demand for electrical energy. It can be seen that the theoretical values are close to the experimental values or to the values collected in real time. This proves that the method of extrapolation by evaluating sunshine on the horizontal plane can be adopted.

Table 5. *Comparison of the results using localities data.*

Methods	Muidere	Youaye	Hoyo	Bougaye
RMSE	3.025	2.025	0.235	0.254
MARE	0.254	0.224	0.235	0.568
MBE	0.365	0.024	0.324	0.845
MAE	4.215	5.021	0.254	1.023
R^2	0.712	0.975	0.908	0.881

8. Conclusion

The results obtained by computing the coefficient of determination, the MAE, the RMSE of the MBE and the MARE, allow us to demonstrate not only the performance of the proposed method, but also the effectiveness of the approach for the evaluation and implementation of a large-scale solar photovoltaic system. The global exploitation of sunshine has enabled us to determine the photovoltaic solar power for the different localities of Hoyo, Youaye, Bougaye and Muidere in the event of the implementation of a large-scale photovoltaic array in the selected localities.

In the Youaye locality, the RMSE = 2.025 obtained, shows the importance of implementing a photovoltaic generator to meet the demand for electrical energy. The same applies to Muidere, where abundant sunshine provides an opportunity to install a photovoltaic generator with a capacity of up to 5.8 MW. In Hoyo, on the other hand, there is not enough sunshine to meet the population's demand for a capacity of over 4MW.

The aim is not only to carry out a horizontal but also an inclined evaluation of the teaching, in order to gain an overall view of the development of a high-capacity photovoltaic power plant capable of supplying all the isolated localities in the Far North region. Once this has been done, it will be possible to determine whether a wind generator is required, depending on the availability of wind. A wind generator could be combined with a photovoltaic generator to provide a valid response to the demand for electrical energy from populations without electricity. This is because these localities are not supplied by the northern interconnected grid, even though they have significant photovoltaic energy potential.

Abbreviations

THD	Total Harmonic Distortion
MPPT	Maximum Power Point Tracking
PVG	Photovoltaic Generators

IEEE	Institute of Electrical and Electronics Engineers
P&O	Perturb and Observe
PWM	Pulse Width Modulation
PLL	Phase-locked Loop

Conflicts of Interest

The authors declare no conflicts of interest.

References

[1] K. Hasan, M. M. Othman, S. T. Meraj, M. Ahmadipour, M. S. H. Lipu, and M. Gitizadeh, "A Unified Linear Self-Regulating Method for Active/Reactive Sustainable Energy Management System in Fuel-Cell Connected Utility Network," *IEEE Access*, vol. 11, pp. 21612–21630, 2023, https://doi.org/10.1109/ACCESS.2023.3249483

[2] A. Thawko, A. Eyal, and L. Tartakovsky, "Experimental comparison of performance and emissions of a direct-injection engine fed with alternative gaseous fuels," *Energy Convers. Manag.*, vol. 251, p. 114988, Jan. 2022, https://doi.org/10.1016/J.ENCONMAN.2021.114988

[3] P. Tiam Kapen, B. A. Medjo Nouadje, V. Chegnimonhan, G. Tchuen, and R. Tchinda, "Techno-economic feasibility of a PV/battery/fuel cell/electrolyzer/biogas hybrid system for energy and hydrogen production in the far north region of cameroon by using HOMER pro," *Energy Strateg. Rev.*, vol. 44, p. 100988, Nov. 2022, https://doi.org/10.1016/J.ESR.2022.100988

[4] F. Mumtaz, N. Z. Yahaya, S. T. Meraj, N. S. S. Singh, M. S. Rahman, and M. S. Hossain Lipu, "A High Voltage Gain Interleaved DC-DC Converter Integrated Fuel Cell for Power Quality Enhancement of Microgrid," *Sustain. 2023, Vol. 15, Page 7157*, vol. 15, no. 9, p. 7157, Apr. 2023, https://doi.org/10.3390/SU15097157

[5] B. S. Varun Sai *et al.*, "An efficient MPPT techniques for inter-harmonic reduction in grid connected hybrid wind and solar energy systems," *Heliyon*, vol. 10, no. 5, Mar. 2024, https://doi.org/10.1016/j.heliyon.2024.e27312

[6] D. K. Patel, D. Singh, and B. Singh, "A comparative analysis for impact of distributed generations with electric vehicles planning," *Sustain. Energy Technol. Assessments*, vol. 52, p. 101840, Aug. 2022, https://doi.org/10.1016/J.SETA.2021.101840

[7] R. Djidimbé, B.-P. Ngoussandou, D. K. Kidmo, Kitmo, M. Bajaj, and D. Raidandi, "Optimal sizing of hybrid Systems for Power loss Reduction and Voltage improvement using PSO algorithm: Case study of Guissia Rural Grid," *Energy Reports*, vol. 8, pp. 86–95, Nov. 2022, https://doi.org/10.1016/J.EGYR.2022.06.093

[8] Kitmo, G. B. Tchaya, and N. Djongyang, "Optimization of the photovoltaic systems on the North Cameroon interconnected electrical grid," *Int. J. Energy Environ. Eng. 2021*, pp. 1–13, Oct. 2021, https://doi.org/10.1007/S40095-021-00427-8

[9] B.-P. Ngoussandou *et al.*, "Optimal Placement and Sizing of Distributed Generations for Power Losses Minimization Using PSO-Based Deep Learning Techniques," *Smart Grid Renew. Energy*, vol. 14, no. 9, pp. 169–181, Oct. 2023, https://doi.org/10.4236/SGRE.2023.149010

[10] J. C. Beltrán, A. J. Aristizábal, A. López, M. Castaneda, S. Zapata, and Y. Ivanova, "Comparative analysis of deterministic and probabilistic methods for the integration of distributed generation in power systems," *Energy Reports*, vol. 6, pp. 88–104, Feb. 2020, https://doi.org/10.1016/J.EGYR.2019.10.025

[11] Yaouba *et al.*, "An Experimental and Case Study on the Evaluation of the Partial Shading Impact on PV Module Performance Operating Under the Sudano-Sahelian Climate of Cameroon," *Front. Energy Res.*, vol. 0, p. 967, Aug. 2022, https://doi.org/10.3389/FENRG.2022.924285

[12] B.-P. Ngoussandou *et al.*, "Optimal energy scheduling method for the North Cameroonian interconnected grid in response to load shedding," *Sustain. Energy Res. 2023 101*, vol. 10, no. 1, pp. 1–25, Sep. 2023, https://doi.org/10.1186/S40807-023-00084-X

[13] S. Usha, P. Geetha, R. Palanisamy, Kitmo, and Y. B. Jember, "Analysis of torque controlling strategies of interior permanent magnet synchronous machine in hybrid electric vehicle," *SN Appl. Sci.*, vol. 5, no. 12, pp. 1–11, Dec. 2023, https://doi.org/10.1007/S42452-023-05563-W/TABLES/4

[14] Y. Xu and C. Singh, "Power System Reliability Impact of Energy Storage Integration With Intelligent Operation Strategy," *IEEE Trans. Smart Grid*, vol. 5, no. 2, pp. 1129–1137, Mar. 2014, https://doi.org/10.1109/TSG.2013.2278482

[15] B.-P. Ngoussandou et alK., G. B. TCHAYA, N. Djongyang, S. Alphonse, and D. K. KAOGA, "Optimization of the smart grids connected using an improved P&O MPPT algorithm and parallel active filters," *J. Sol. Energy Res.*, vol. 6, no. 3, pp. 814–828, Jul. 2021, https://doi.org/10.22059/JSER.2021.320173.1196

[16] A. F. Minai *et al.*, "Evolution and role of virtual power plants: Market strategy with integration of renewable based microgrids," *Energy Strateg. Rev.*, vol. 53, p. 101390, May 2024, https://doi.org/10.1016/J.ESR.2024.101390

[17] B. Bogno *et al.*, "Enhancing the power quality in radial electrical systems using optimal sizing and selective allocation of distributed generations," *PLoS One*, vol. 19, no. 12, p. e0316281, Dec. 2024, https://doi.org/10.1371/JOURNAL.PONE.0316281

[18] Kitmo, R. Djidimbé, D. K. Kidmo, G. B. Tchaya, and N. Djongyang, "Optimization of the power flow of photovoltaic generators in electrical networks by MPPT algorithm and parallel active filters," *Energy Reports*, vol. 7, pp. 491–505, Nov. 2021, https://doi.org/10.1016/J.EGYR.2021.07.103

[19] Andre, B. K. and Ernest, K. (2025) Experimental Evaluation of Solar Power Plant Performances for the Choice of a Suitable Photovoltaic System. Smart Grid and Renewable Energy, 16, 97-110. https://doi.org/10.4236/sgre.2025.165006

[20] V. G. Gormo, D. K. Kidmo, B. P. Ngoussandou, B. Bogno, D. Raidandi, and M. Aillerie, "Wind power as an alternative to sustain the energy needs in Garoua and Guider, North Region of Cameroon," *Energy Reports*, vol. 7, pp. 814–829, Nov. 2021, https://doi.org/10.1016/J.EGYR.2021.07.059

[21] M. F. Elnaggar *et al.*, "Optimal sizing and power losses reduction of photovoltaic systems using PSO and LCL filters," *PLoS One*, vol. 19, no. 4, p. e0301516, Apr. 2024, https://doi.org/10.1371/JOURNAL.PONE.0301516

[22] T. Jeyaseelan, P. Ekambaram, J. Subramanian, and T. Shamim, "A comprehensive review on the current trends, challenges and future prospects for sustainable mobility," *Renew. Sustain. Energy Rev.*, vol. 157, p. 112073, Apr. 2022, https://doi.org/10.1016/J.RSER.2022.112073.

[23] H. Salvarli, M. S. Salvarli, H. Salvarli, and M. S. Salvarli, "For Sustainable Development: Future Trends in Renewable Energy and Enabling Technologies," *Renew. Energy - Resour. Challenges Appl.*, Sep. 2020, https://doi.org/10.5772/INTECHOPEN.91842

[24] N. Bello-Pierre *et al.*, "Energy Efficiency in Periods of Load Shedding and Detrimental Effects of Energy Dependence in the City of Maroua, Cameroon," *Smart Grid Renew. Energy*, vol. 14, no. 4, pp. 61–71, Apr. 2023, https://doi.org/10.4236/SGRE.2023.144004

[25] P. Rani, V. Parkash, and N. K. Sharma, "Technological aspects, utilization and impact on power system for distributed generation: A comprehensive survey," *Renew. Sustain. Energy Rev.*, vol. 192, p. 114257, Mar. 2024, https://doi.org/10.1016/J.RSER.2023.114257

[26] B. E. K. Nsafon, A. B. Owolabi, H. M. Butu, J. W. Roh, D. Suh, and J. S. Huh, "Optimization and sustainability analysis of PV/wind/diesel hybrid energy system for decentralized energy generation," *Energy Strateg. Rev.*, vol. 32, p. 100570, Nov. 2020, https://doi.org/10.1016/j.esr.2020.100570

[27] T. E. K. Zidane *et al.*, "Grid-connected Solar PV power plants optimization: A review," *IEEE Access*, 2023, https://doi.org/10.1109/ACCESS.2023.3299815

[28] S. K. Sahu, K. Mazumdar, B. Kitmo, Y. B. Jember, and S. Das, "Design and investigation of InGaAs/InP/InAlAs MOSFET with optimized switching efficiency," *IEEE Access*, pp. 1–1, 2024, https://doi.org/10.1109/ACCESS.2024.3401851

[29] A. Boussaibo, A. D. Pene, K. , A. Boussaibo, A. D. Pene, and K. , "Optimal Sizing and Power Losses Reduction of Photovoltaic Systems Using PVsyst Software," *J. Power Energy Eng.*, vol. 12, no. 7, pp. 23–38, Jul. 2024, https://doi.org/10.4236/JPEE.2024.127002

[30] Kitmo, G. B. Tchaya, and N. Djongyang, "Optimization of hybrid grid-tie wind solar power system for large-scale energy supply in Cameroon," *Int. J. Energy Environ. Eng. 2022*, pp. 1–13, Nov. 2022, https://doi.org/10.1007/S40095-022-00548-8

[31] G. Byanpambé *et al.*, "A modified fractional short circuit current MPPT and multicellular converter for improving power quality and efficiency in PV chain," *PLoS One*, vol. 19, no. 9, p. e0309460, Sep. 2024, https://doi.org/10.1371/JOURNAL.PONE.0309460

[32] R. A. Nascimento, A. lvaro B. Neto, Y. S. De Freitas Bezerra, H. A. D. Do Nascimento, L. Dos Santos Lucena, and J. E. De Freitas, "A new hybrid optimization approach using PSO, Nelder-Mead Simplex and Kmeans clustering algorithms for 1D Full Waveform Inversion," *PLoS One*, vol. 17, no. 12, p. e0277900, Dec. 2022, https://doi.org/10.1371/JOURNAL.PONE.0277900

[33] T. N. Thanh, P. V. Minh, K. D. Trung, and T. Do Anh, "Study on Performance of Rooftop Solar Power Generation Combined with Battery Storage at Office Building in Northeast Region, Vietnam," *Sustain. 2021, Vol. 13, Page 11093*, vol. 13, no. 19, p. 11093, Oct. 2021, https://doi.org/10.3390/SU131911093

[34] A. H. M. Hanif, M. S. Jadin, N. Sulaiman, A. S. Abdullah, and L. W. Jun, "Improving the Effect of Non-uniform Thermal Distribution and Electrical Mismatch for PV Panel During Partial Shading Condition," *Lect. Notes Electr. Eng.*, vol. 770, pp. 1067–1080, 2022, https://doi.org/10.1007/978-981-16-2406-3_78

[35] C. A. Wankouo Ngouleu, Y. W. Koholé, F. C. V. Fohagui, and G. Tchuen, "Techno-economic analysis and optimal sizing of a battery-based and hydrogen-based standalone photovoltaic/wind hybrid system for rural electrification in Cameroon based on meta-heuristic techniques," *Energy Convers. Manag.*, vol. 280, p. 116794, Mar. 2023, https://doi.org/10.1016/J.ENCONMAN.2023.116794